ON THE TAILORING OF RADIALLY FGM HOLLOW SPHERES, CYLINDERS AND DISKS

STEFAN SOROHAN , DAN MIHAI CONSTANTINESCU*, DRAGOS ALEXANDRU APOSTOL

Abstract. Homogeneous and isotropic thick spheres, cylinders, and thin disks subjected to constant internal and/or external pressures are not easily designed in an economical way due to the localized occurrence of maximum equivalent stress. It has been analytically shown that using a radial functionally graded material (FGM) can enhance the design process by ensuring that the maximum shear stress or the circumferential stress component remains constant along the radius of the body. This problem is an inverse one. An isotropic FGM in linear static analysis can be defined by two elastic constants: Young's modulus $E(r)$ and Poisson's ratio $\nu(r)$. In this study, focusing on mechanical loading, the conditions for the existence of a solution for $E(r)$ in the inverse problem are derived, assuming a constant Poisson's ratio and using two commonly applied stress criteria in design. Additionally, the advantages of employing FGMs over homogeneous materials are demonstrated by comparing the maximum equivalent stresses in both cases.

Keywords: thick-walled shell, functionally graded material (FGM), material tailoring, equal stress structure.

1. INTRODUCTION

In the current literature, for simple symmetrically loaded functionally graded material (FGM) structures, such as spheres, thick-walled tubes, or thin disks, stress conditions have been established under which certain stress components – such as in-plane shear stress or circumferential stress – reach constant values throughout the entire geometry. In some specific cases, these stress conditions are equivalent to the maximum equivalent stress criterion. The necessary distributions of Young's modulus $E(r)$, assuming an isotropic FGM and a constant Poisson's ratio $\nu(r)$ = const., have been derived in studies such as those by Guven and Baykara [1]

Department of Strength of Materials, National University of Science and Technology "Politehnica" Bucharest, Splaiul Independenţei 313, Bucharest 060042, Romania
[*] Corresponding author, Institute of Solid Mechanics, Romanian Academy, 15 Constantin Mille str., Bucharest, Romania

Ro. J. Techn. Sci. – Appl. Mechanics, Vol. 69, N^{os} 2–3, P. 167–190, Bucharest, 2024

DOI:10.59277/RJTS-AM.2024.2-3.05

and Nie *et al*. [2]. In the case of orthotropic FGMs, where the Young's moduli are assumed to be proportional to each other, the distributions of $E(r)$ have been obtained by Leissa and Vagins [3] and Nie *et al*. [4]. These approaches are based on the solutions to inverse problems in the elastic theory of inhomogeneous bodies. Other stress conditions, related to classical strength theories and used in solving inverse problems, are presented in works by Andreev [5, 6], Andreev *et al*. [7], and Andreev and Potekhin [8].

In practice, for an isotropic FGM, most problems involve both $E(r)$ and $\nu(r)$ as variables, and these properties are not always well-known or easily defined. To address such relatively complex problems, common approaches assume specific forms of variation for $E(r)$ such as power law, exponential law, or parabolic variation – while typically keeping $\nu(r)$ = const. Analytical closed-form solutions are often obtained for certain loading cases, primarily focusing on mechanical loads, though some also incorporate thermal effects. These solutions are typically presented as direct problems in the current literature. Most studies focus on the sensitivity analysis of the parameters defining the chosen variation laws for $E(r)$ and $\nu(r)$. However, only a few papers investigate cases close to the condition of constant circumferential stress, and none address situations approaching constant in-plane shear stress. This paper seeks to explain this apparent gap by discussing the existence of such solutions and provides observations on how effectively the optimized $E(r)$ function can be described using the selected variation law.

Analytical closed-form solutions for thick-walled spheres with a constant Poisson's ratio ($\nu(r)$ = const.) have been presented by several researchers, including Eslami *et al*. [9], Nayak *et al*. [10], Zamani Nejad *et al*. [11], Bayat *et al*. [12], and Karami *et al*. [13]. Additionally, numerical solutions assuming $\nu(r)$ = const. were provided by Hadi *et al*. [14], while Li *et al*. [15] derived solutions for cases where both $E(r)$ and $\nu(r)$ vary arbitrarily, either continuously or piecewise.

For thick-walled cylinders, analytical closed-form solutions are also available under the assumption that $\nu(r)$ = const., as discussed in references [16–19]. A unified approach for analytical and numerical solutions for both cylinders and spheres is presented in Xie *et al*. [20]. Furthermore, numerical solutions for the case of constant Poisson's ratio can be found in [21–24]. For cases involving arbitrarily varying material properties in graded hollow cylinders, both numerical and analytical solutions are available in [25, 26]. Finally, for thin disks, most analytical or numerical solutions consider factors such as rotating loads and uniform or variable thickness, with results obtained for a constant Poisson's ratio in studies [27–29].

For functionally graded hollow spheres, cylinders, and disks subjected to uniform internal pressure, where the material properties vary in the radial direction, general numerical solutions have been obtained by Tutuncu and Temel [30]. They used the fifth-order Runge–Kutta method to solve the problem, considering both Young's modulus and Poisson's ratio as arbitrary functions of the radial coordinate.

Closed-form solutions for functionally graded circular hollow cylinders and spheres subjected to internal and external pressures, where the material is assumed to be incompressible and linearly elastic with $\nu(r)$ = const. = 0.5, were derived by Batra [31, 32]. These studies revealed that the optimal circumferential stress in both the cylinder and the sphere is constant when the shear modulus varies linearly with the radial direction. To achieve constant in-plane shear stress throughout the thickness of the cylinder and sphere, the shear modulus must vary as r^2 for the cylinder and r^3 for the sphere. Further investigations on functionally graded isotropic and incompressible elastic hollow spheres were conducted by Iaccarino and Batra [33] and Benslimane [34].

This work focuses on the design optimization of functionally graded spheres, cylinders, and disks by uniformizing two of the most used stress conditions found in the literature. The goal is to tailor these structures to achieve desired stress distributions, enhancing their performance under mechanical loading.

The paper is organized in five sections, as follows. In section two, the paper briefly presents the analytical solutions of tailoring pressurized FGM spheres, cylinders and disks for the two most used stress conditions in literature: in-plane shear stress and circumferential stress to be constant. Then, in section three, the conditions for the existence of practical solutions obtained in section two, are presented. In section four, the efficiency of the use of a FGM axi-symmetrical body instead of the homogeneous one is discussed. Comments on the obtained results are also presented. The paper concludes with some general conclusions in the last section.

2. ANALYTICAL OPTIMAL SOLUTIONS

We consider a sphere, cylinder, or disk with an inner radius a and an outer radius b, subjected to internal pressure p_a and external pressure p_b (Fig. 1). The material of the structure is assumed to be a functionally graded material (FGM) with radial symmetry, meaning the material properties vary only in the radial direction from the center to the outer surface.

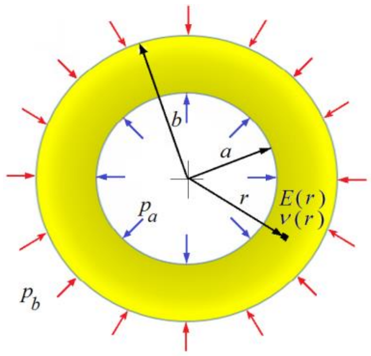

Fig. 1 – Isotropic inhomogeneous FGM sphere/cylinder/disk.

In the spherical and cylindrical symmetric case, the radial and circumferential stresses are $\sigma_r(r)$ and $\sigma_\theta(r)$ and neglecting the body forces, the equilibrium equation must be satisfied as [35]

$$\frac{\mathrm{d}\sigma_r}{\mathrm{d}r}+\frac{\chi}{r}(\sigma_r-\sigma_\theta)=0, \tag{1}$$

where the shape factor $\chi = 2$ for spherical bodies and $\chi = 1$ for cylindrical bodies. For the sake of a simple notation, here and below the radial dependence of variables $\sigma_r(r)$ and $\sigma_\theta(r)$ is omitted in the formal notation.

For radially symmetric deformation, the only nonzero component of the displacement vector is $u_r = u(r)$. The strain-displacement equations are

$$\varepsilon_r=\frac{\mathrm{d}u}{\mathrm{d}r};\quad \varepsilon_\theta=\frac{u}{r}, \tag{2,a,b}$$

and corresponding strains, ε_r and ε_θ, must satisfy the compatibility equation

$$\varepsilon_r=\frac{\mathrm{d}}{\mathrm{d}r}(r\varepsilon_\theta). \tag{3}$$

The first two stress-strain relations may be written in matrix form

$$\begin{Bmatrix}\varepsilon_r\\ \varepsilon_\theta\end{Bmatrix}=\frac{1}{E}\begin{bmatrix}c_{11} & c_{12}\\ c_{21} & c_{22}\end{bmatrix}\begin{Bmatrix}\sigma_r\\ \sigma_\theta\end{Bmatrix}, \tag{4,a,b}$$

where Hookean coefficients are given in Table 1. Supplementary, the equation

$$\varepsilon_z=\frac{1}{E}\left[\sigma_z-\nu(\sigma_r+\sigma_\theta)\right], \tag{5}$$

is used for cylinders and disks, assuming plane strain $(\varepsilon_z=0)$ or plane stress $(\sigma_z=0)$, respectively.

Table 1

Coefficients in Eq. (4) for particular axi-symmetrical bodies

Hookean coefficients in Eqs. (4)	Sphere	Cylinder plane strain $(\varepsilon_z=0)$	Disk plane stress $(\sigma_z=0)$
c_{11}	1	$1-\nu^2$	1
c_{12}	-2ν	$-\nu\,(1+\nu)$	$-\nu$
c_{21}	$-\nu$	$-\nu\,(1+\nu)$	$-\nu$
c_{22}	$1-\nu$	$1-\nu^2$	1

It is to be noticed that for all the three geometries from Table 1 is fulfilled the condition $c_{11}+c_{12}-c_{21}-c_{22}=0$, which is further used in solving equation (9). In designing FGM bodies in current literature, the most used stress conditions, i.e. $\sigma_r-\sigma_\theta=\text{const.}$ and $\sigma_\theta=\text{const.}$ are named in this work as Opt 1 and Opt 2, respectively.

2. 1. Stress condition Opt 1

Substituting the stress condition

$$\sigma_r-\sigma_\theta=C_0=\text{const.}, \tag{6}$$

in the equilibrium equation (1) and by using boundary conditions $\sigma_r(a)=-p_a$ and $\sigma_r(b)=-p_b$, the radial and circumferential stresses are obtained as:

$$\sigma_r(r)=\frac{p_a\log\frac{b}{r}-p_b\log\frac{a}{r}}{\log\frac{a}{b}}, \tag{7}$$

$$\sigma_\theta(r)=\frac{p_a\left(\chi\log\frac{b}{r}-1\right)-p_b\left(\chi\log\frac{a}{r}-1\right)}{\chi\log\frac{a}{b}}. \tag{8}$$

The radial stress obtained only from the equation of equilibrium (1) and which satisfies relation (6), has the same expression for all the analyzed bodies (sphere, cylinder, disk). It is to be underlined that the stress distributions depend only on the geometry and loading, being independent of the material properties. For cylinder (plane strain), the axial stresses are obtained from relation (5), that is $\sigma_z=\nu(\sigma_r+\sigma_\theta)$.

If the constitutive equations for a material as (4) are introduced in (3), results the differential equation

$$\frac{\mathrm{d}}{\mathrm{d}r}\left(r\frac{1}{E}\left[c_{21}\sigma_r+c_{22}\sigma_\theta\right]\right)=\frac{1}{E}\left(c_{11}\sigma_r+c_{12}\sigma_\theta\right). \tag{9}$$

By introducing (7) and (8) in (9) and solving for $E(r)$, with the notations

$$n_1=\chi\left(\frac{c_{21}}{c_{22}}+1\right),\quad n_2=1+\frac{c_{11}c_{22}-c_{12}c_{21}}{\chi\left(c_{21}+c_{22}\right)^2}, \tag{10}$$

results the expression which describes the variation of the modulus of elasticity as a function of geometry, loading, and Poisson’s ratio.

$$E(r) = C_1 \left\{ p_a \left[1 + n_1 \log\left(\frac{r}{b}\right) \right] - p_b \left[1 + n_1 \log\left(\frac{r}{a}\right) \right] \right\}^{n_2}. \tag{11}$$

In expression (11), C_1 is a constant of integration, which can be usually established by imposing/choosing a value for E in the interval $a \le r \le b$, in most of the cases at one of the two extremes of r variation.

The values of the parameters n_1 and n_2 can be estimated by using notations (10) and Table 1, and are presented in Table 2.

By introducing (7) and (8) in (6) results

$$\sigma_r - \sigma_\theta = C_0 = \frac{p_a - p_b}{\chi \log \frac{a}{b}} = \text{cont.} \tag{12}$$

The displacements field results from relation (2,b), that is $u = \varepsilon_\theta r$ in which ε_θ is obtained from (4,b) by replacing the stresses from equations (7) and (8) and Young's modulus expression from equation (11).

Table 2

Coefficients in Eq. (11) for particular axi-symmetrical bodies if the stress condition (6) i.e. Opt 1, is enforced

Coefficients	Sphere (χ = 2)	Cylinder (χ = 1)	Disk (χ = 1)
n_1	$\frac{2(1-2\nu)}{1-\nu}$	$\frac{1-2\nu}{1-\nu}$	$1-\nu$
n_2	$\frac{3(1-\nu)}{2(1-2\nu)}$	$\frac{2(1-\nu)}{1-2\nu}$	$\frac{2}{1-\nu}$

2. 2. Stress condition Opt 2

Similarly as described in the previous section, for the condition

$$\sigma_\theta = D_0 = \text{const.}, \tag{13}$$

it results the stress distributions:

$$\sigma_r(r) = p_a \frac{a^\chi}{b^\chi - a^\chi} \left[1 - \left(\frac{b}{r}\right)^\chi \right] - p_b \frac{b^\chi}{b^\chi - a^\chi} \left[1 - \left(\frac{a}{r}\right)^\chi \right], \tag{14}$$

$$\sigma_\theta(r) = \frac{p_a a^\chi - p_b b^\chi}{b^\chi - a^\chi}. \tag{15}$$

It is noticed that the radial stress from equation (14), obtained only from the condition of equilibrium (1) and by imposing relation (13), has different variations for the sphere, where χ =2 and for cylinder, respectively disk, where χ = 1. Again, for this case also, the distribution of stress depends only on the geometry and loading.

The expression which describes the variation of the modulus of elasticity as a function of geometry, loading, and Poisson's ratio results

$$E(r) = C_2 \left\{ p_a \left(\frac{a}{b}\right)^{\chi} \left[1 + n_1 \left(\frac{b}{r}\right)^{\chi}\right] - p_b \left[1 + n_1 \left(\frac{a}{r}\right)^{\chi}\right] \right\}^{n_2}, \tag{16}$$

where C_2 is an integration constant and n_1 and n_2 are different from the previous case and are given in Table 3.

Table 3

Coefficients in Eq. (16) for particular axi-symmetrical bodies if the stress condition (13), i.e. Opt 2, is enforced

Coefficients	Sphere (χ = 2)	Cylinder (χ = 1)	Disk (χ = 1)
n_1	$\frac{\nu}{1-2\nu}$	$\frac{\nu}{1-2\nu}$	$\frac{\nu}{1-\nu}$
n_2	$\frac{\nu-1}{2\nu}$	$\frac{\nu-1}{\nu}$	$-\frac{1}{\nu}$

3. CONDITIONS FOR THE EXISTENCE OF SOLUTIONS

The distribution of the Young's modulus obtained in relation (11) for the condition of optimization Opt 1 and, respectively, in relation (16) for Opt 2 must describe variations which fit in a relatively small interval because, practically, the variations obtained for a FGM material are of the order of units [36]. The variations of $E(r)$ are dependent of: *i*) geometry: a, b and χ; *ii*) boundary conditions, that is considered loading, in this paper only pressures p_a and p_b; and respectively *iii*) Poisson's ratio $\nu(r)$ which intervenes in calculating n_1 and n_2. If Poisson's ratio is considered constant then $E(r) > 0$ is a function defined only by the geometry and loading.

It is known that for the two conditions of optimization with the bodies and loading considered in this paper $E(r)$ lead to an uniform increasing variations as a function of r. That is, the minimum value is $E(r=a) = E_a$ and, respectively the maximum value is $E(r=b) = E_b$.

3. 1. Case of Opt 1

For the beginning we consider relation (11) which corresponds to the condition of optimization (6). If $E(r = a) = E_a$ is imposed, then from (11) we obtain C_1 as

$$C_1 = \frac{E_a}{\left\{ p_a \left[1 + n_1 \log\left(\frac{a}{b}\right) \right] - p_b \right\}^{n_2}}, \tag{17}$$

which introduced in (11) gives as a result

$$E(r) = E_a \left\{ \frac{p_a \left[1 + n_1 \log\left(\frac{r}{b}\right) \right] - p_b \left[1 + n_1 \log\left(\frac{r}{a}\right) \right]}{p_a \left[1 + n_1 \log\left(\frac{a}{b}\right) \right] - p_b} \right\}^{n_2}. \tag{11'}$$

If we consider ν = const., and a uniform variation of $E(r)$, then $E(r = b) = E_b$ and from (11') we obtain

$$\frac{E_b}{E_a} = \left\{ \frac{p_a - p_b \left[1 + n_1 \log\left(\frac{b}{a}\right) \right]}{p_a \left[1 - n_1 \log\left(\frac{b}{a}\right) \right] - p_b} \right\}^{n_2}. \tag{18}$$

For $p_a \neq 0$, equation (18) is rewritten in the form

$$\frac{E_b}{E_a} = \left\{ \frac{1 - \left(\frac{p_b}{p_a}\right) \left[1 + n_1 \log\left(\frac{b}{a}\right) \right]}{\left[1 - n_1 \log\left(\frac{b}{a}\right) \right] - \left(\frac{p_b}{p_a}\right)} \right\}^{n_2}. \tag{18'}$$

Similarly, for $p_b \neq 0$, equation (18) becomes

$$\frac{E_b}{E_a} = \left\{ \frac{\left(\frac{p_a}{p_b}\right) - \left[1 + n_1 \log\left(\frac{b}{a}\right) \right]}{\left(\frac{p_a}{p_b}\right) \left[1 - n_1 \log\left(\frac{b}{a}\right) \right] - 1} \right\}^{n_2}. \tag{18''}$$

Equations (18') and (18") can be used as to estimate the ratio E_b / E_a (a measure of the variation range of the Young's modulus), function of the ratio of the two radii b / a (a measure of the relative thickness of the walls) in the condition of choosing constant values of the pressure loadings p_b / p_a or p_a / p_b, and respectively the Poisson's ratio ν. In practice, if $E_b > E_a$, the value of the ratio of the two moduli is in the order of units as is also the ratio b / a, for which, in most cases found in the literature, b / a = 10 is not exceeded.

Relations (18), (18') and (18") are valid for sphere, cylinder and disk when imposing the condition $\sigma_r - \sigma_\theta = C_0 = \text{const.}$

3. 2. Case of Opt 2

We consider relation (16) which corresponds to the condition of optimization (13), notated as Opt 2. Similarly, as above, is imposed $E(r = a) = E_a$, and then from (16) is obtained C_2 which being introduced in (16) leads to

$$E(r) = E_a \left\{ \frac{p_a \left(\frac{a}{b}\right)^{\chi} \left[1 + n_1 \left(\frac{b}{r}\right)^{\chi}\right] - p_b \left[1 + n_1 \left(\frac{a}{r}\right)^{\chi}\right]}{p_a \left(\frac{a}{b}\right)^{\chi} \left[1 + n_1 \left(\frac{b}{a}\right)^{\chi}\right] - p_b (1 + n_1)} \right\}^{n_2} . \tag{16'}$$

If ν = const., and a uniform variation of $E(r)$, than the value $E(r = b) = E_b$ results from (16') and we obtain

$$\frac{E_b}{E_a} = \left\{ \frac{p_a \left(\frac{a}{b}\right)^{\chi} (1 + n_1) - p_b \left[1 + n_1 \left(\frac{a}{b}\right)^{\chi}\right]}{p_a \left(\frac{a}{b}\right)^{\chi} \left[1 + n_1 \left(\frac{b}{a}\right)^{\chi}\right] - p_b (1 + n_1)} \right\}^{n_2} . \tag{19}$$

For $p_a \neq 0$ equation (19) can be rewritten and a function of the ratios p_b / p_a and b / a, respectively ν which intervenes in n_1 and n_2 from Table 3. If it is necessary, the case $p_b \neq 0$ can be also considered.

The variation range of the Young's modulus, given by the ratio E_b / E_a as a function of the relative thickness of the body walls, specified through the radii ratio b / a, in the condition of choosing p_b / p_a = 0 and p_a / p_b = 0, with constant Poisson's ratio value from 0.01 to 0.49, is presented in the following figures as design curves. In Fig. 2 the variations are obtained for a sphere loaded with internal pressure p_a for the two stress conditions Opt 1 and Opt 2.

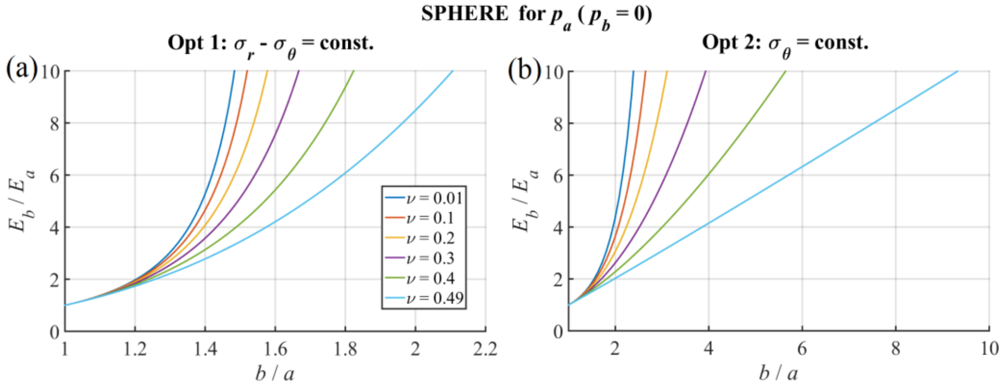

Fig. 2 – Practical design curves of the optimized solutions for an internally pressurized sphere at different Poisson's ratios: a) for $\sigma_r - \sigma_\theta$ = const.; b) for σ_θ = const.

From Fig. 2a. it is noticed that an internally pressurized sphere can be designed as a FGM with a variation range $E(r)$ relatively reduced, that is bellow E_b / E_a < 10 in the condition Opt 1, only for spheres for which b / a is relatively small (that is maximum around 2), as compared to the use of condition Opt 2 (Fig. 2b), where the design can be done for much thicker spheres, as b/a can exceed a value of 5, or even more, for quasi-incompressible materials. More than that it is noticed that a constant value of Poisson's ratio has a significant influence on the domain of existence of the solution, as the ratios b/a increase together with the increase of ν.

If a pressurized cylinder or a disk is considered, the shape of Fig. 2 is similar. As compared to the sphere the design domain for b/a increases for the cylinder with above 30% but bellow about 50% for Opt 1, and for the case Opt 2, the increase of the design domain given by b/a is more pronounced for low contraction coefficients, and can increase with maximum 40%. For the disk, as compared to the cylinder the ratio b/a decreases slightly, being more pronounced for greater contraction coefficients. As an example, for the case Opt 1 with ν = 0.3 and E_b / E_a =10, b/a for an internally pressurized sphere is 1.67, for the pressurized cylinder becomes 2.32, and for a disk is 2.20.

In Fig. 3 the variations of the design curves are presented for a sphere loaded with external pressure p_b for the two stress conditions Opt 1 and Opt 2.

In Fig. 3a it is observed that an externally pressurized sphere can be designed as a FGM with a variation range for $E(r)$ (ratio E_b / E_a up to 10) in the condition Opt 1, for spheres with b/a greater than for the sphere with internal pressure, that is around 5 for small contraction coefficients. In the condition Opt 2 the design can be done without any restrictions in wall thickness as b/a can exceed without any problems the value of 10. Additionally, also for this load case, it is noticed that the constant value chosen for the Poisson's ratio has a great influence on the domain of existence of the solution, especially for Opt 1, as contrary to the case of internal pressure, the b/a values increase with the decrease of ν.

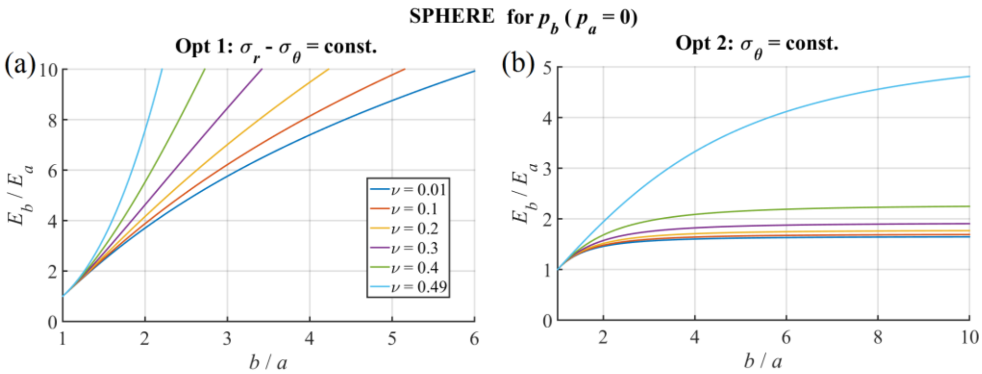

Fig. 3 – Practical design curves of the optimized solutions for an externally pressurized sphere at different Poisson's ratios: a) for $\sigma_r - \sigma_\theta$ = const.; b) for σ_θ = const.

If it is considered an externally pressurized cylinder or disk the shape of the curves from Fig. 3 is similar. Compared to the sphere, the design domain for b/a for a cylinder increases with over 40% but less than about 50% for the case Opt 1. If condition Opt 2 is considered, comparing to the sphere, the range of variation of E_b / E_a for the cylinder increases with about 60% for coefficients of contraction close to 0.3, but even so, the design of cylinders as to uniformize the circumferential stress can be done in a very large design domain of b/a. The curves of the existing solutions for the disk, compared to the cylinder, are very close for both conditions of optimization, with the exception of case Opt 2 for quasi-incompressible materials. Just as an example of comparison, for the case Opt 1 with ν = 0.3 and b/a =3 for the externally pressurized sphere, the ratio E_b / E_a is 8.46, for the cylinder 5.50, and for the disk 5.10. For Opt 2 with ν = 0.3 and b/a = 6 for external pressure on a sphere ratio E_b / E_a is 1.87, for the cylinder 2.81, and for the disk 2.61.

If the ratio of the external towards the internal pressure is $p_b / p_a = 2$ and ν is constant through the wall thickness, in Fig. 4 are presented for a cylinder and the two stress conditions the obtained design curves from which are extracted the particular conditions for the existence of the solutions. For this loading case and $\nu < 0.4$ solutions are valid for very large values b / a, that is very thick cylinders.

If the ratio becomes $p_b / p_a = -2$, then the design curves for a valid solution are presented in Fig. 5, drawing the conclusion that for some loading cases the influence of Poisson's ratio is much weaker. Similar curves, but differently positioned, are to be obtained for the sphere and the disk.

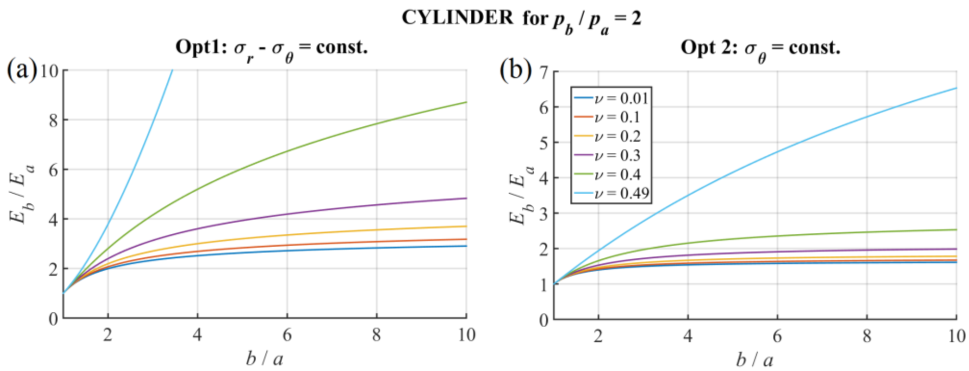

Fig. 4 – Practical design curves of the optimized solutions for a pressurized cylinder with $p_b / p_a = 2$ at different Poisson's coefficient values: a) for $\sigma_r - \sigma_\theta$ = const.; b) for σ_θ = const.

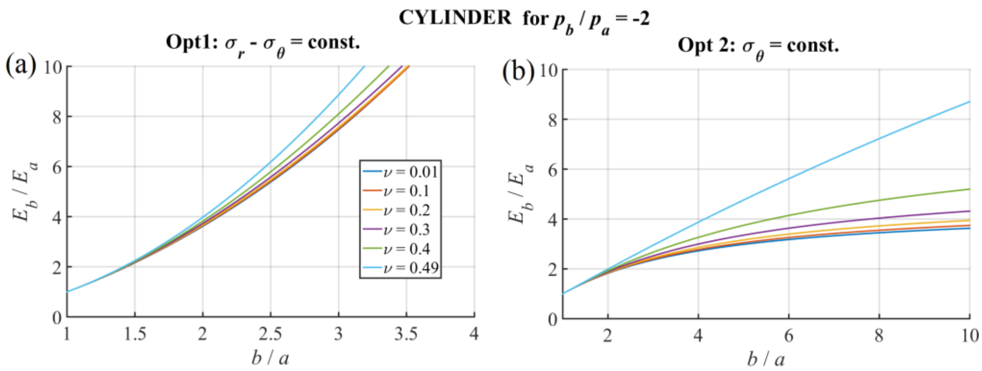

Fig. 5 – Practical design curves of the optimized solutions for a pressurized cylinder with $p_b / p_a = -2$ at different Poisson's coefficient values: a) for $\sigma_r - \sigma_\theta$ = const.; b) for σ_θ = const.

When using Opt 2, if the material is incompressible, that is $\nu \to 0.5$, for the sphere and the cylinder the first bisector is obtained, that is an affine variation, result which is confirmed and presented by Batra [31]. Similarly, for Opt 1, for cylinders and spheres, the shear modulus (here Young's modulus), must be proportional to r^2 and r^3, respectively [32]. These statements are not valid for the disk.

As to show that the loading, given by p_b / p_a, is influencing significantly the curves for the existence of the solution, in Fig. 6 are presented the design curves showing the existence of the solution if $\nu = 0.3$ = const. and different loading cases given by p_b / p_a .

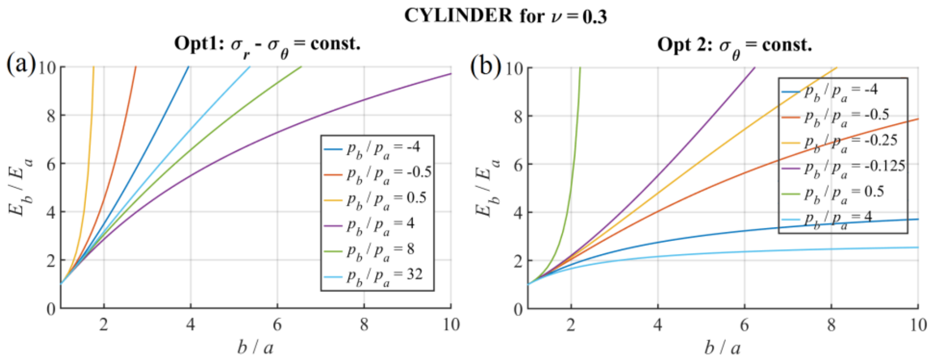

Fig. 6 – Practical design curves of the optimized solutions as a function of the loading p_b / p_a for a cylinder with ν = 0.3 = const.: a) for $\sigma_r - \sigma_\theta$ = const.; b) for σ_θ = const.

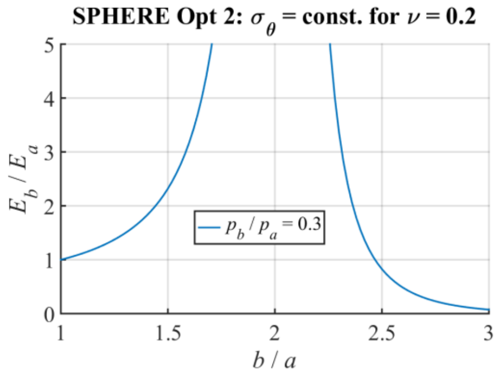

Fig. 7 – Curves for the existence of a particular solution for a sphere and the condition of optimization Opt 2 in which the right curve does not lead to a monotonic solution for $E(r)$.

As in this paper it is not possible to present all loading cases, it is recommended to use relations (18) and (19) as to obtain the curves for a particular design. It is to be mentioned that the use of these relations is not always sufficient because one has to verify that the relations obtained for $E(r)$ lead to monotonic and continuous functions. So, the uniform variation of $E(r)$ has to be validated by representing equations (11') or (16'), after establishing the geometry, the loading, and respectively choosing the constant value of Poisson's ratio. There are situations when for certain input data the ratio E_b / E_a remains in a relatively narrow domain, but the variation of $E(r)$ may give significant variations between a and b. As an example, in Fig. 7 is represented a particular case for the condition of optimization Opt 2, for a loading with p_b / p_a = 0.3 and ν = 0.2. The left plot is correct as function $E(r)$ shows an increasing trend, but the right plot obtained by using the theoretical solution for $E(r)$ is not a monotonic function, as having a vertical asymptote, $E(r) \to \infty$ between a

and b; although E_b / E_a has apparently a value of units in most of the shown interval (Fig. 7), the $E(r)$ tends to infinity towards its middle.

4. THE EFFICIENCY OF USING FGM

The use of a FGM instead of homogeneous material with $E(r)$ = const. is usually justified due to the reduction of the stress components in bodies made from such a material. As to justify this assertion, in this paper are presented some results based on the relations of calculus presented previously. As for making a comparison, the relations for calculating the stresses in a homogeneous material are needed, and these are presented hereby in a condensed form.

4. 1. Homogeneous and isotropic material

From the classical textbooks on strength of materials or theory of elasticity [35], or from equations (1) – (5), the stresses distribution in a homogeneous and isotropic material are resulting as

$$\sigma_r = p_a \frac{a^{\chi+1}}{\left(b^{\chi+1} - a^{\chi+1}\right)}\left(1 - \frac{b^{\chi+1}}{r^{\chi+1}}\right) - p_b \frac{b^{\chi+1}}{\left(b^{\chi+1} - a^{\chi+1}\right)}\left(1 - \frac{a^{\chi+1}}{r^{\chi+1}}\right), \tag{20}$$

$$\sigma_\theta = p_a \frac{a^{\chi+1}}{\left(b^{\chi+1} - a^{\chi+1}\right)}\left(1 + \frac{1}{\chi}\frac{b^{\chi+1}}{r^{\chi+1}}\right) - p_b \frac{b^{\chi+1}}{\left(b^{\chi+1} - a^{\chi+1}\right)}\left(1 + \frac{1}{\chi}\frac{a^{\chi+1}}{r^{\chi+1}}\right), \tag{21}$$

mentioning that for a sphere χ = 2 and $\sigma_\theta = \sigma_\varphi$, for a cylinder χ = 1 and $\sigma_z = \nu\left(\sigma_r + \sigma_\theta\right)$, and for a disk χ = 1 and $\sigma_z = 0$.

As based on the stresses distribution the displacements $u(r)$ or strains by using equations (1) – (5) can be obtained.

4. 2. Equivalent stresses

Up to now, in this work were established the conditions of existence for a FGM for particular conditions of distribution of the stresses, named Opt 1 and Opt 2. However, usually in practice is important the distribution of the equivalent stresses. As follows, there are presented the calculus relations of the equivalent stresses based on the classical strength theories used for isotropic materials.

The normal stresses in a body (radial, circumferential, axial) are sorted as principal stresses $\sigma_1 \geq \sigma_2 \geq \sigma_3$. According to Timoshenko [37] and Yu [38], if we assume that the allowable stresses in tension and compression are the same in absolute value, then the classical strength theories are:

I. according to maximum stress theory (Rankine)

$$\sigma_{eqv}^{I} = \max\left(\left|\sigma_1\right|, \left|\sigma_3\right|\right); \tag{22}$$

where symbol | | was used for absolute value.

II. according to maximum strain theory (Saint Venant)

$$\sigma_{eqv}^{II} = \max\left(\left|\sigma_1 - \nu\left(\sigma_2 + \sigma_3\right)\right|, \left|\sigma_3 - \nu\left(\sigma_1 + \sigma_2\right)\right|\right); \tag{23}$$

III. according to maximum shear theory (Tresca)

$$\sigma_{eqv}^{III} = \sigma_1 - \sigma_3; \tag{24}$$

V. according to maximum distortion strain energy theory (von Mises)

$$\sigma_{eqv}^{V} = \frac{1}{\sqrt{2}}\sqrt{\left(\sigma_1 - \sigma_2\right)^2 + \left(\sigma_2 - \sigma_3\right)^2 + \left(\sigma_3 - \sigma_1\right)^2}. \tag{25}$$

For a sphere, because the two of three principal stresses are always equals, it results $\sigma_{eqv}^{III} = \sigma_{eqv}^{V} = \left|\sigma_\theta - \sigma_r\right|$. So, for a sphere, the design according to condition (6) or Opt 1 is the same in obtaining constant equivalent stresses according to (24) and (25). If $\left|\sigma_\theta\right| \geq \left|\sigma_r\right|$, then using (22) it results $\sigma_{eqv}^{I} = \left|\sigma_\theta\right|$ and the condition (13) or Opt 2 is the same as (22).

It has to be underlined that in general, for axi-symmetrical FGM bodies, it is difficult to identify the stress components $\sigma_r, \sigma_\theta, \sigma_z$ as being principal stresses and the correct use of relations (22) – (25) in the theoretical analyses. Because in a FGM body the stress σ_θ may change the sign along the radius, the calculus relations of the equivalent stresses may become complicated and do not correspond anymore to the homogeneous isotropic one. In Table 4 is presented only a simple load case (internally presurized axi-symmetrical bodies discussed in this paper) as to show that the apparently simple statement "or" mentioned there leads to significant complications in the analytical approach. It is also possible to obtain relations for bodies of large dimensions, as *b* / *a* can reach high values. A complex loading case is presented [5] for a FGM cylinder which needs establishing three options during the calculations.

Table 4

Principal and equivalent stresses for an internal pressurized FGM body ($p_a > 0$ and $p_b = 0$)

Body	Principal stresses $\sigma_1 \geq \sigma_2 \geq \sigma_3$	Maximum stress σ^{I}_{eqv}	Maximum shear stress σ^{III}_{eqv}	Maximum distortion strain energy (von Mises) σ^{V}_{eqv}
Sphere	$\sigma_1 = \sigma_\theta$ $\sigma_2 = \sigma_\varphi = \sigma_\theta$ $\sigma_3 = \sigma_r$	$\text{abs}(\sigma_\theta)$ or $\text{abs}(\sigma_r)$	$\sigma_\theta - \sigma_r$	$\sigma_\theta - \sigma_r$
Infinite long cylinder	$\sigma_1 = \sigma_\theta$ $\sigma_2 = \sigma_z$ or $\sigma_2 = \sigma_r$ $\sigma_3 = \sigma_r$ or $\sigma_3 = \sigma_z$	$\text{abs}(\sigma_\theta)$ or $\text{abs}(\sigma_r)$	$\sigma_\theta - \sigma_r$ or $\sigma_\theta - \sigma_z$	$\sqrt{\frac{1}{2}\begin{bmatrix}(\sigma_\theta - \sigma_z)^2 \\ +(\sigma_z - \sigma_r)^2 \\ +(\sigma_r - \sigma_\theta)^2\end{bmatrix}}$
Hollow disk	$\sigma_1 = \sigma_\theta$ or $\sigma_1 = 0$ $\sigma_2 = 0$ or $\sigma_2 = \sigma_\theta$ $\sigma_3 = \sigma_r$	$\text{abs}(\sigma_\theta)$ or $\text{abs}(\sigma_r)$	$\sigma_\theta - \sigma_r$ or $-\sigma_r$	$\sqrt{\sigma_r^2 + \sigma_\theta^2 - \sigma_r \sigma_\theta}$

4. 3. Comparison of the results obtained for fgm versus homogeneous

Based on the relations (7), (8), (11), (14−16) and (20−25) which describe the distribution of the radial and circumferential stresses as well as the distribution of $E(r)$ for the two stress conditions Opt 1 and Opt 2 in FGM bodies but also in homogeneous bodies, it is possible to obtain graphical representations which can highlight the advantages of using FGMs. Other variables, as deformations were calculated based on the general relations (1) – (5).

For two identical bodies (spheres, cylinders, disks) one from FGM and the other homogeneous, with $E_{Hom} = E_{\max,Inh}$, both with ν = const., are presented in parallel the distributions of relative measures (Young's modulus, displacements, stresses) in the same loading conditions for the two variants of optimization Opt 1 and Opt 2, of the $E(r)$ distributions in FGM. It is to be mentioned that it is considered that $p = \max(\text{abs}(p_a), \text{abs}(p_b))$ and $\nu = 0.3$, and that for the three types of bodies different b / a values were chosen as to fulfill the conditions of the existence of the solution, as presented in section 3.

4. 3. 1. Internally pressurized sphere

For spheres loaded with interior pressure, in Fig. 8 are presented the radial variations of the normalized Young's modulus E / E_{Hom}; normalized deformation $u \cdot E_{Hom}$ / $(a \cdot p)$; normalized radial stress σ_r / p ; normalized circumferential stress

σ_θ / p and normalized equivalent stresses according to maximum stress and maximum shear stress if the design is based on the Opt 1 stress condition. The similar curves are also presented for the second design condition of the stress distribution Opt 2 in Fig. 9.

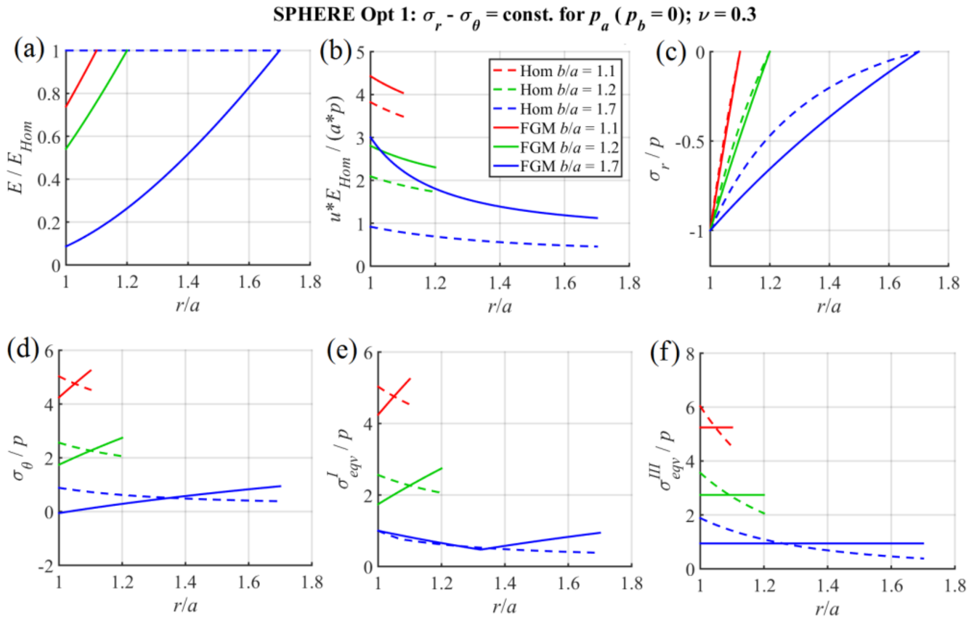

Fig. 8 – Distributions of normalized quantities for a series of three homogeneous and FGM internally pressurized spheres if the stress distribution in FGM is enforced to be according to Opt 1 and Poisson's ratio ν = 0.3 = const.

As the FGM spheres are less rigid at the interior than those made from a homogeneous material (Fig. 8a) their displacements are a little bit greater (Fig. 8b) than those corresponding to the homogeneous material. The radial stresses are a little bit greater in the central part of the wall (Fig. 8c) and the circumferential ones are greater at the exterior of the sphere (Fig. 8d). For the homogeneous material the circumferential stresses are always greater at the interior of the sphere and always positive. For FGM the circumferential stresses can be negative at the interior of the sphere if $b/a > \sqrt{e} \approx 1.649$. Also for FGM, the maximum circumferential stresses are greater than the maximum radial ones, if $b/a < \sqrt[4]{e} \approx 1.284$. Using the I[st] maximum stress theory, the FGM sphere does not lead to smaller stresses compared with the homogeneous sphere (Fig. 8e), while for the III[rd] and V[th] strength theories the FGM leads to smaller stresses (Fig. 8f). To determine the effect of the optimized model of the inhomogeneous equal-stress structure, Andreev (2012) introduced the *efficiency ratio*

$$\beta = \frac{p_{\max}^{Inh}}{p_{\max}^{Hom}} = \frac{\sigma_{eqv,\max}^{Hom}}{\sigma_{eqv,\max}^{Inh}}, \tag{26}$$

which shows how many times the external loads on the body can be increased, in comparison with the homogeneous analogue. The efficiency ratio for b / a = 1.1 in this case (Fig. 8f) is 1.15, whereas for b / a = 1.7 it is around 2.00, but in this last case E_b / E_a = 11.56, which is a very high value from practical point of view (Fig. 8a). The conclusion is that only for very thick spheres the efficiency ratio is high. Unfortunately, in this particular load case and if ν = 0.3, the maximum practical ratio b/a is limited to around 1.7. This limit may be increased to around 2.1 (Fig. 2a) if the material is incompressible.

By analyzing Fig. 9a it is to be observed that the design domain b / a in the condition Opt 2 has increased compared to optimization condition Opt 1. There are feasible solutions for b/a < 3.5 − 4 if ν = 0.3, but this domain can be enlarged if an incompressible material is used, as it is to be noticed from Fig. 2b. Qualitatively, the resulting displacement and radial stress distributions are similar to the ones obtained with condition Opt 1.

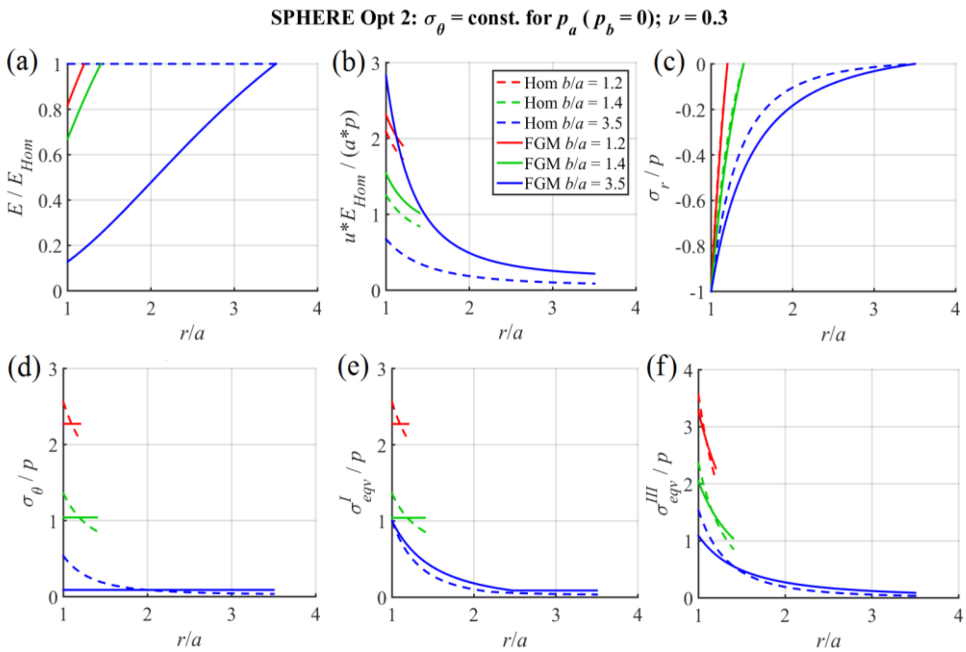

Fig. 9 – Distributions of normalized quantities for a series of three homogeneous and FGM internally pressurized spheres if the stress distribution in FGM is enforced to be according to Opt 2 and Poisson's ratio ν = 0.3 = const.

For a FGM the circumferential stresses are constant and positive and greater in absolute value than the radial ones if $b/a < \sqrt{2} \approx 1.414$ (Fig. 9d). Using I[st] strength theory, the FGM sphere leads to smaller stresses than the homogeneous one (Fig. 9e), only if $b / a < 1.414$, where the efficiency ratio is maximum 1.32. With the III[rd] and the V[th] strength theories, the FGM sphere leads to smaller stresses (Fig. 9f) for any b/a, but the efficiency ratio β is maximum 1.41 if $b/a = 3.5$, and for $\nu = 0.3 =$ const. it results $E_b / E_a = 7.8$. If we accept a ratio $E_b / E_a = 10$, for an incompressible material it results, at the limit, $\beta = 1.5$.

This conclusion is very important: for thick spheres, which are internally pressurized and designed in stress condition Opt 2 with $\nu =$ const., the efficiency ratio never results greater than 1.5, although the circumferential stresses can be reduced for more than 6 times, see for example Fig. 9d, for $b/a = 3.5$, or even for about 50 times if $\nu \to 0.5$.

4. 3. 2. Externally pressurized sphere

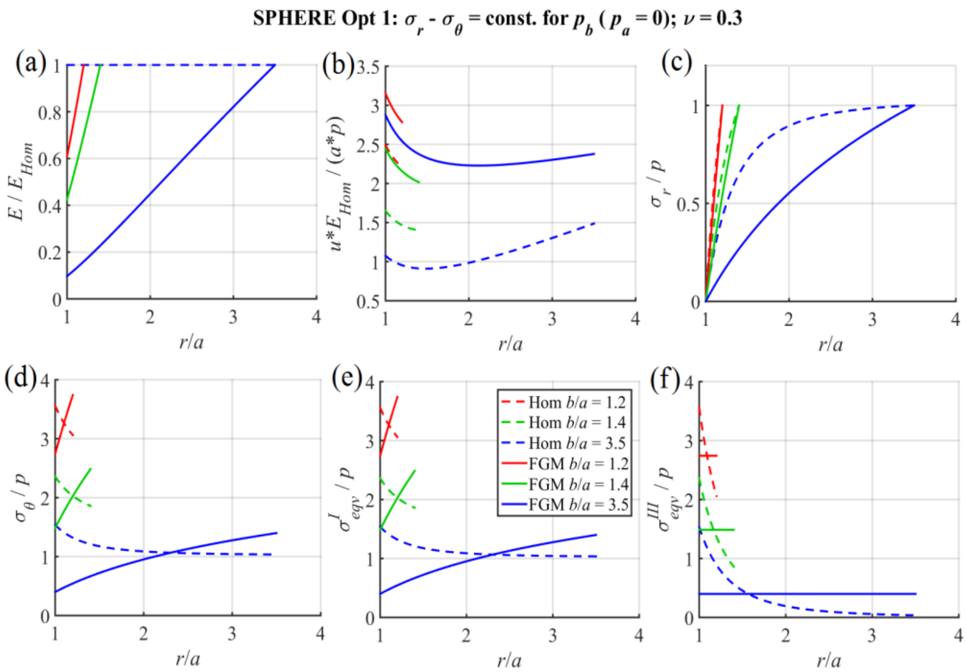

Fig. 10 – Distributions of normalized quantities for a series of three homogeneous and FGM externally pressurized spheres if the stress distribution in FGM is enforced according to Opt 1 and Poisson's ratio ν = 0.3 = const.

For spheres loaded only with an external pressure, in Fig. 10 are shown the variations of the same variables as in the previous subchapter, if the design is based on the Opt 1 stress condition, and in Fig. 11 if the design is based on the Opt 2 stress condition. In these plots, the external pressure is considered negative.

If we consider the loading as being external pressure (Fig. 3a and Fig. 10a), for the design condition Opt 1 and $\nu = 0.3 = \text{const.}$, for $b/a = 3.5$ results $E_b / E_a = 10.3$ and $\beta = 3.85$ for the III[rd] and V[th] theories, and for the I[st] strength theory, the efficiency ratio is only $\beta = 1.1$. When $\nu \to 0$, for $b/a = 6.5$, results $E_b / E_a = 10.3$ and $\beta = 5.63$ for theories III and V, and for theory I, we obtain only $\beta = 1.19$.

From Fig. 11 it is noticed that for wide design ranges of b / a (very thick spheres), E_b / E_a is surprisingly reduced (about 1.88 for $b/a = 6.0$) as compared to the condition Opt 1, but also the efficiencies β are significantly reduced, as about 1.09; 1.16 and 1.47 for the strength theories and the ratios considered in this figure as $b/a = 1.2$; 1.4 and 6.0.

Also for external pressure, but for the design condition Opt 2 and $\nu = 0.3 = \text{const.}$ (Fig. 3b), for $b/a = 10$, results $E_b / E_a = 1.9$ and $\beta = 1.49$ for all strength theories. When $\nu \to 0$ or $\nu \to 0.5$, regardless the ratio b/a, and the used strength theory, it is obtained that the efficiency ratio never results larger than 1.5.

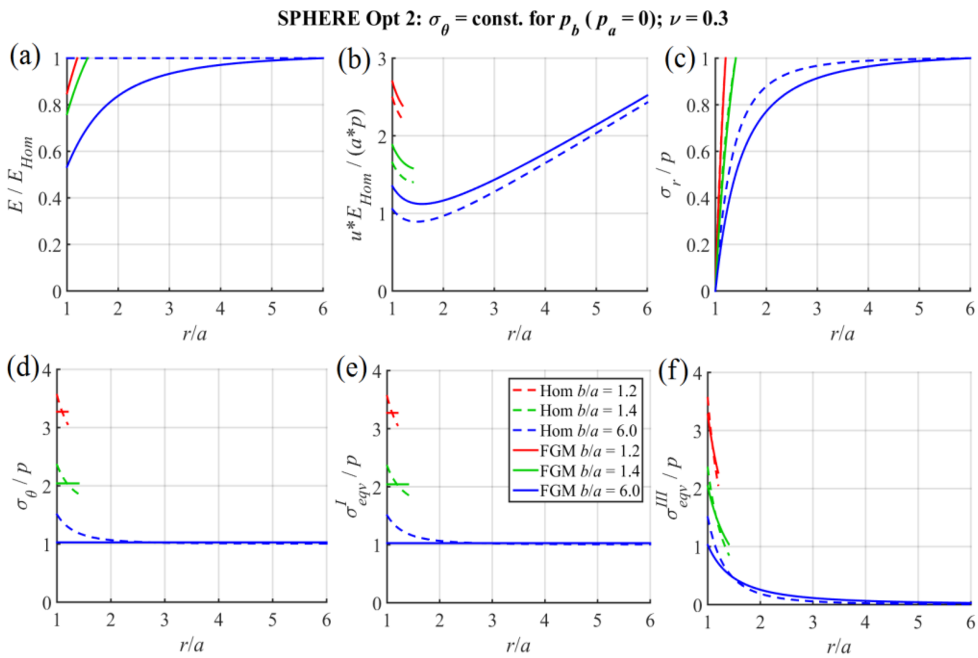

Fig. 11 – Distributions of normalized quantities for a series of three homogeneous and FGM externally pressurized spheres if the stress distribution in FGM is enforced according to Opt 2 and Poisson's ratio ν = 0.3 = const.

4. 3. 3. Cylinder and disk

For a cylinder or a disk loaded only with internal pressure the results are similar with those obtained for a sphere, but the design domain may be extended and the presence or absence of the axial (longitudinal) stresses σ_z can complicate the analytical analysis.

For example, for a cylinder, if *b*/*a* = 2.2, stress distribution according to Opt 1 and $\nu = 0.3$ it results $E_b / E_a = 8.13$ and the efficiency ratio results $\beta = 1.20$ for I[st] strength theory, $\beta = 1.99$ for the III[rd] theory and $\beta = 1.94$ for the V[th] theory. For a disk, if *b*/*a* = 2.2, stress distribution according to Opt 1 and $\nu = 0.3$, results $E_b / E_a =$ 9.91 and the efficiency ratio $\beta = 1.20$ for I[st] strength theory, $\beta = 1.99$ for III[rd] theory, and $\beta = 1.73$ for V[th] strength theory.

These discussions can be extended to different scenarios, and if the goal is to achieve a practical design with an increased value of β\betaβ, it is recommended to plot the relevant variables using the relations established earlier.

Most studies in the open literature focus on the material tailoring problem to achieve a desired distribution of a specific stress component across the cross-section. However, in practice, damage typically occurs due to the combined effects of all components of the stress tensor, according to a given strength theory. Therefore, it is essential to tailor the design based on an appropriate strength criterion, rather than focusing solely on a particular stress condition.

5. CONCLUSIONS

For the three types of analyzed bodies – spheres, thick-walled cylinders, and thin disks – subjected only to internal and external pressures, and for the design conditions of $\sigma_r - \sigma_\theta = \text{const.}$ and $\sigma_\theta = \text{const.}$ with $\nu(r)$ = const. analytical expressions for the variation of $E(r)$ were derived in a unified form. Specifically, for the condition $\sigma_r - \sigma_\theta = \text{const.}$, the relation (11) was obtained, and for $\sigma_\theta = \text{const.}$, the relation (16) was derived.

Given that, for a fixed geometry and loading conditions, and assuming $\nu(r)$ = const., the ratio E_b / E_a remains constant and $E(r)$ increases uniformly with *r*, it was possible to analyze the conditions under which solutions exist using the ratios E_b / E_a and *b*/*a*. From a practical perspective, it was found that these design conditions are applicable primarily for geometries where the ratio *b*/*a* is relatively small. The influence of assuming a constant Poisson’s ratio on the range of variation of E_b / E_a was also examined. It was observed that, in certain loading cases and stress conditions, the effect of Poisson's ratio can be negligible (for example Fig. 5a), but in most cases, the variation of v has a significant impact and should be considered in the design process.

The analytical solutions for both homogeneous and FGM bodies allowed for a direct comparison, in dimensionless form, of the efficiency of using FGMs in design, under the assumptions of constant Poisson's ratio and the two uniform stress conditions. This comparison revealed graphical representations demonstrating the enhanced loading capacity of FGM structures relative to homogeneous ones, assuming that the strength of the FGM is comparable to that of the homogeneous material. It was also shown that, depending on the strength theory applied, the FGM structure does not always outperform the homogeneous structure in terms of performance.

Acknowledgements. This work was supported by a grant, contract no.11/06.10.2023, code 112, from the National Program for Research of the National Association of Technical Universities – GNAC ARUT 2023.

Received on 19 November, 2024

REFERENCES

1. GUVEN, U., BAYKARA, C., *On Stress Distributions in Functionally Graded Isotropic Spheres Subjected to Internal Pressure*, Mech. Res. Commun., **28**, *3*, pp. 277–281, 2001.
2. NIE, G.J., ZHONG, Z., BATRA, R.C., *Material tailoring for functionally graded hollow cylinders and spheres*, Compos. Sci. Technol., **71**, *5*, pp. 666–673, 2011.
3. LEISSA, A.W., VAGINS, M., *The design of orthotropic materials for stress optimization*, Int. J. Solids Struct., **14**, pp. 517–526, 1978, https://doi.org/10.1016/0020-7683(78)90014-8.
4. NIE, G.J., ZHONG, Z., BATRA, R.C., *Material tailoring for orthotropic elastic rotating disks*, Compos. Sci. Tech., **71**, pp. 406–414, 2011, https://doi.org/10.1016/j.compscitech.2010. 12.010
5. ANDREEV, V.I., *Optimization of thick-walled shells based on solutions of inverse problems of the elastic theory for inhomogeneous bodies*, In Computer Aided Optimum Design in Engineering XII, Eds. Hernández, S., Brebbia, C.A., Wilde, W.P., 189–202, 2012, WIT Press.
6. ANDREEV, V.I., *Inverse problems of the inhomogeneous theory of elasticity for thick-walled shells*, Int. J. Comput. Methods Exp. Meas., **2**, pp. 202–216, 2014.
7. ANDREEV, V.I., POTEKHIN, I.A., *Equal strength and equal stress structures. Models and reality*, Adv. Eng. Res., **102**, pp. 232–236, 2017.
8. ANDREEV, V.I., CHEPURNENKO, A.S., JAZYEV, B.M., *Model of equal-stressed cylinder based on the Mohr failure criterion*, Adv. Mater. Res., **887**, pp. 869–872, 2014.
9. ESLAMI, M.R., BABAEI, M.H., POULTANGARI, R., *Thermal and mechanical stresses in a functionally graded thick sphere*, Int. J. Press. Vessels Pip., **82**, pp. 522–527, 2005, https://doi.org/10.1016/j.ijpvp.2005.01.002.
10. NAYAK, P, MONDAL, S.C., NANDI A, *Stress, strain and displacement of a functionally graded thick spherical vessel*, Int. J. Eng. Sci. Tech., **3**, pp. 2659–2671, 2011.
11. ZAMANI NEJAD, M., ABEDI, M., LOTFIAN, M.H., GHANNAD, M., *An exact solution for stresses and displacements of pressurized FGM thick-walled spherical shells with exponential-varying properties*, J. Mech. Sci., **26**, *12*, pp. 4081–4087, 2012.

12. BAYAT, Y., GHANNAD, M., TORABI, H., *Analytical and numerical analysis for the FGM thick sphere under combined pressure and temperature loading*, Arch. Appl. Mech., **82**, pp. 229–242, 2011.
13. KARAMI, K., ABEDI, M., ZAMANI NEJAD, M., LOTFIAN, M. H., *Elastic analysis of heterogeneous thick-walled spherical pressure vessels with parabolic varying properties*, Front. Mech. Eng., **7**, pp. 433–438, 2012, https://doi.org/10.1007/s11465-012-0336-1.
14. HADI, A., RASTGOO, A., ZAMANI NEJAD, M., *Effect of exponentially-varying properties on displacements and stresses in pressurized functionally graded thick spherical shells with using iterative technique*, J. Solid Mech., **6**, pp. 366–377, 2014.
15. Li, X.F., Peng, X.L., Kang, Y.A., *Pressurized hollow spherical vessels with arbitrary radial nonhomogeneity*, AIAA J., **47**, pp. 2262–2265, 2009, https://doi.org/10.2514/1.41995.
16. HORGAN, C.O., CHAN, A.M., *The pressurized hollow cylinder or disk problem for functionally graded isotropic linearly elastic materials*, J. Elast., **55**, pp. 43–59, 1999, https://doi.org/ 10.1023/A:1007625401963.
17. TUTUNCU, N., OZTURK, M., *Exact solutions for stresses in functionally graded pressure vessels*, Compos. Part B-Eng., **32**, *8*, pp. 683–686, 2001.
18. SHI, P., XIE, J., *Revisiting classic problems of exact solutions for stresses in functionally graded pressure vessels*, Mech. Res. Commun., **110**, 103609, 2020.
19. BENSLIMANE, A., BENCHALLAL, R., MAMMERI, S., METHIA, M., KHADIMALLAH, M.A., *Investigation of displacements and stresses in thick-walled FGM cylinder subjected to thermo-mechanical loadings*, Int. J. Comput. Methods Eng. Sci. Mech., **22**, pp. 138–149, 2020, https://doi.org/10.1080/15502287.2020.1853853.
20. XIE, J, HAO, S, WANG, W., SHI, P., *Analytical solution of stress in functionally graded cylindrical/spherical pressure vessel*, Arch. Appl. Mech., **91**, pp. 3341–3363, 2021, https://doi.org/10.1007/s00419-021-01970-w.
21. CHEN, Y.Z., LIN, X.Y., *Elastic analysis for thick cylinders and spherical pressure vessels made of functionally graded materials*, Comput. Mater. Sci., **44**, *2*, pp. 581–587, 2008.
22. CHEN, Y.Z., LIN, X.Y., *An alternative numerical solution of thick-walled cylinders and spheres made of functionally graded materials*, Comput. Mater. Sci., **48**, *2*, pp. 640–647, 2010.
23. Saeedi, S., Kholdi, M., Loghman, A., Ashrafi, H., Arefi, M., *Thermo-elasto-plastic analysis of thick-walled cylinder made of functionally graded materials using successive approximation method*, Int. J. Press. Vessels Pip., **194**, 104481, 2021, https://doi.org/10.1016/j.ijpvp.2021. 104481.
24. YARIMPABUÇ, D., *Nonlinear Thermal Stress Analysis of Functionally Graded Thick Cylinders and Spheres*, Iran. J. Sci. Technol. Trans., **45**, pp. 655–663, 2021, https://doi.org/10.1007/ s40997-020-00395-0.
25. LI, X-F., PENG, X-L. *A pressurized functionally graded hollow cylinder with arbitrarily varying material properties*, J. Elast., **96**, pp. 81–95, 2009, https://doi.org/10.1007/s10659-009-9199-z.
26. NĂSTĂSESCU, V., MARZAVAN, S., *Functionally graded thick-walled tubes analysis by numerical methods*, Heliyon, **10**, e27309, 2024, https://doi.org/10.1016/ j.heliyon.2024. e27309.
27. ZENKOUR, A.M., *Analytical solutions for rotating exponentially-graded annular disks with various boundary conditions*, Int. J. Struct. Stab. Dy., **5**, pp. 557–577, 2005. https://doi.org/ 10.1142/S0219455405001726.
28 BAYAT, M., SALEEM, M., SAHARI, B.B., HAMOUDA, A.M.S., MAHDI, E., *Analysis of functionally graded rotating disks with variable thicknes*s, Mech. Res. Commun., **35**, pp. 283–309, 2008, https://doi.org/10.1016/j.mechrescom.2008.02.007.
29. ÇALLIOĞLU, H., SAYER, M., DEMIR, E., *Elastic–plastic stress analysis of rotating functionally graded discs*, Thin-Walled Struct., **94**, pp. 38–44, 2015, http://dx.doi.org/ 10.1016/j.tws. 2015.03. 016.
30. TUTUNCU, N., TEMEL, B., *A novel approach to stress analysis of pressurized FGM cylinders, disks and spheres*, Compos. Struct., **91**, *3*, pp. 385–390, 2009.

31. BATRA, R.C., *Optimal Design of Functionally Graded Incompressible Linear Elastic Cylinders and Spheres*, AIAA J., **46**, *8*, pp. 2050–2056, 2008.
32. BATRA, R.C., *Material tailoring and universal relations for axisymmetric deformations of functionally graded rubberlike cylinders and spheres*, Math. Mech. Solids, **16**, *7*, pp. 729–738, 2011.
33. IACCARINO, G.L., BATRA, R.C., *Analytical solution for radial deformations of functionally graded isotropic and incompressible second-order elastic hollow spheres*, J. Elast., **107**, pp. 179–197, 2012, https://doi.org/10.1007/s10659-011-9350-5.
34. BENSLIMANE, A., *Nonlinear stress analysis of rubber-like thick-walled sphere using different constitutive models*, Mater. Today Proc., **53**, pp. 46–51, 2022, https://doi.org/10.1016/j.matpr.2021.12.284.
35. TIMOSHENKO, S.P., GOODIER, J.N., *Theory of elasticity*, MC Graw-Hill, New York, 1951.
36. El-Galy, I.M., Saleh, B.I., Ahmed, M.H., *Functionally graded materials classifications and development trends from industrial point of view*, SN Appl. Sci., **1**, 1378, 2019, https://doi.org/10.1007/s42452-019-1413-4
37. TIMOSHENKO, S.P., *Strength of materials, Part II, Advanced Theory and Problems,* Second Edition (Ninth printing), D. Van Nostrand Company, Inc., New York, 1947.
38. YU, M., *Advances in strength theories for materials under complex stress state in the 20th Century*, Appl. Mech. Rev., **55**, pp. 169–218, 2002, https://doi.org/10.1115/1.1472455.